Bubble Nucleation in Superheated Liquid–Liquid Emulsions

C. T. AVEDISIAN[1] AND R. P. ANDRES[2]

School of Engineering and Applied Science, Princeton University, Princeton, New Jersey 08540

Received April 11, 1977; accepted October 7, 1977

An investigation of the process by which bubbles form in superheated liquid–liquid emulsions is reported. A theoretical model for the rate of bubble nucleation is developed that is valid for any binary liquid system. Because of the interesting "microexplosion" phenomenon postulated to occur during combustion of fuel/water emulsions, special attention is focused on hydrocarbon/water/surfactant mixtures. The model predicts that in these systems nucleation takes place at the interface between the two liquids but that the vapor bubbles rest entirely within the hydrocarbon phase.

The maximum superheat limits of emulsions containing 83% by volume hydrocarbon (benzene, *n*-decane, *n*-dodecane, *n*-tetradecane, and *n*-hexadecane), 15% water and 2% surfactant were measured experimentally at 1 atm and found to be in good agreement with the predictions of the theoretical model. The superheat limits of these emulsions are lower than those of either pure liquid. However, for microexplosion of an emulsified fuel droplet, the superheat limit of the fuel/water emulsion must be less than the boiling point of the fuel. Only the *n*-hexadecane/water emulsion satisfies this criterion at atmospheric pressure.

1. INTRODUCTION

It is almost axiomatic that improvements in atomization and vaporization of high-boiling-point fuels result in cleaner, more efficient combustion. A promising approach in this regard is to emulsify the fuel with water prior to burning (1). The effect of adding water is twofold. First, the water serves as a diluent. It reduces both liquid-droplet and gas-phase temperatures in the flame, thereby moderating undesirable reactions that lead to production of soot and NO_x. Secondly, as first observed by Ivanov and Nefedov (2), emulsified fuel droplets tend to explode when heated, thereby solving the problem of fuel atomization.

This latter "microexplosion" phenomenon has its origin in the volatility difference between the water and the fuel. Since the water is dispersed and isolated in the emulsion as relatively immobile microdroplets, evaporation from the surface of an emulsified fuel drop is primarily from the continuous fuel phase. Thus, when such a drop is heated, its temperature approaches the boiling point of the pure fuel. With a high-boiling point fuel this means that the water becomes superheated. This metastable condition is maintained only as long as no vapor bubbles form within the drop. Each emulsion exhibits a critical maximum temperature, termed its limit of superheat, at which the probability of bubble nucleation becomes appreciable. If the drop temperature reaches this superheat limit, it disintegrates spontaneously, shattered by the internal formation of vapor bubbles and the consequent rapid vaporization of superheated water.

A necessary condition for microexplosion of an emulsified fuel droplet is that the limit of superheat of the emulsion be less than the boiling point of the fuel. In order to make practical use of this condition one must have a theoretical expression for the limit of

[1] Department of Aerospace and Mechanical Sciences.
[2] Department of Chemical Engineering.

0021-9797/78/0643-0438$02.00/0

superheat. Thus, it is necessary to understand the process by which vapor bubbles nucleate in superheated emulsions.

In what follows we will not consider heterogeneous nucleation on solid motes or impurities. We focus instead on the process by which vapor bubbles form homogeneously either within one of the immiscible liquids or at the surface between the two liquids. Since critical size bubbles or nuclei are generally much smaller than the dispersed droplets present in practical emulsions, the interface can be treated as a flat surface. The problem reduces to that of homogeneous bubble nucleation in a system of two immiscible liquids separated by a flat interface.

There have been several studies of bubble nucleation in which a drop of a volatile test liquid is immersed in an immiscible host fluid and is heated until it vaporizes (3–10). Except in the case of water (4), the superheat limits measured in these experiments do not seem to be dependent on the nonvolatile host fluid and are in excellent agreement with a kinetic model for nucleation that assumes bubbles form homogeneously within the test drop.

Moore (3) was the first to consider the effect of the host fluid. He postulated that discrepancies between theory and experiment in the water case were due to nucleation at the surface of the water drop. Moore developed a thermodynamic model for such interfacial nucleation which takes into account the surface tensions of both liquids and the interfacial tension between them. Apfel (9) and Jarvis *et al.* (10) have also studied this problem and have derived kinetic expressions for the rate of bubble nucleation at the interface between a volatile and a nonvolatile liquid. These treatments are in agreement with the few existing experiments but neglect the contribution of the less volatile liquid to bubble growth.

Thus, existing kinetic models for the rate of bubble nucleation in pure liquids and at the interface between a volatile and a nonvolatile liquid are in agreement with the experimental facts. What remains is to extend these theoretical treatments to include cases in which both components of an emulsion are of comparable volatility. In the present paper we formulate such a general theoretical model and compare its predictions with experiment.

2. THERMODYNAMICS OF BUBBLE FORMATION

The minimum work required to form a vapor bubble at a flat liquid–liquid interface is (11)

$$W = V''(p' - p'') + \sum_i n_i''(\mu_i'' - \mu_i') + \sigma_a S_a + \sigma_b S_b - \sigma_{ab} S_{ab}. \quad [1]$$

In this equation V'' is the volume of the bubble; p' is the ambient pressure in the liquid; p'' is the vapor pressure in the bubble; n_i'' is the number of molecules of component i in the bubble; μ_i'' and μ_i' are the chemical potentials of component i in the vapor and in the liquid, respectively; σ_a, σ_b, and σ_{ab} are the surface tensions associated with the respective interfaces; and S_a, S_b, and S_{ab} are the respective interfacial areas (see Fig. 1). The first term in Eq. [1] accounts for the pV work required to form the bubble. The second term represents the chemical work required to introduce n_i'' molecules of species i into the bubble (the summation extends over all species present in the bubble). The last three terms are the work required to create or destroy the respective interfacial surfaces. We implicitly assume in Eq. [1] and in all that follows that the bubble is in thermal and mechanical equilibrium with the surrounding liquid.

The detailed lenticular shape of such a bubble is shown in Fig. 1. A force balance yields

$$\sigma_{ab} = \sigma_a \cos\theta + \sigma_b \cos\psi, \quad [2]$$

and

$$\sigma_a \sin\theta = \sigma_b \sin\psi. \quad [3]$$

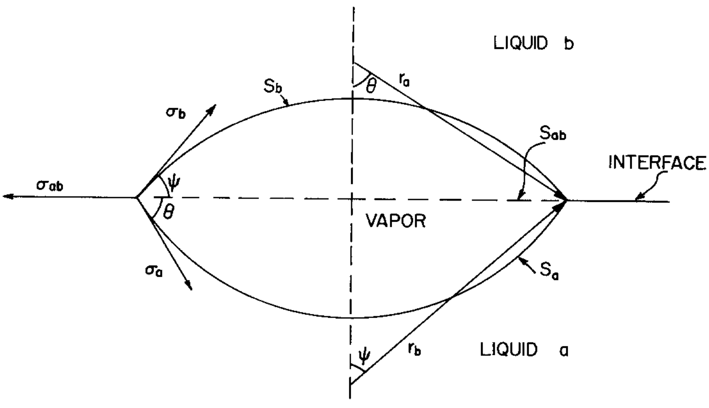

FIG. 1. Geometry of lenticular bubble at a liquid–liquid interface.

Solving these equations one obtains

$$M_a = \cos\theta = \frac{\sigma_a^2 - \sigma_b^2 + \sigma_{ab}^2}{2\sigma_a\sigma_{ab}}, \quad [4]$$

and

$$M_b = \cos\psi = \frac{\sigma_b^2 - \sigma_a^2 + \sigma_{ab}^2}{2\sigma_b\sigma_{ab}}. \quad [5]$$

In addition

$$r_a = 2\sigma_a/(p'' - p') \quad [6]$$

and

$$r_b = 2\sigma_b/(p'' - p'). \quad [7]$$

Equation [1] can be transformed through the use of Eqs. [4]–[7] and straightforward geometrical considerations to yield

$$W = \frac{16}{3}\pi\sigma^3(p'' - p')^{-2} + \sum_i n_i''(\mu_i'' - \mu_i'), \quad [8]$$

where σ is a generalized surface tension which depends on the relative magnitudes of σ_a, σ_b, and σ_{ab}.

The lenticular shape that has been assumed in the derivation of Eq. [8] can exist in mechanical equilibrium only when

$$\sigma_{ab} > |\sigma_a - \sigma_b|. \quad [9]$$

If Eq. [9] is not satisfied, the bubble is spherical in shape and rests entirely within the liquid with the lower surface tension. Thus, there are three distinct possibilities:

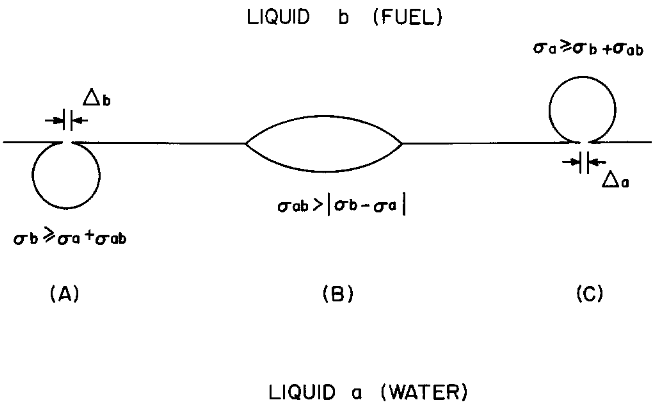

FIG. 2. Possible locations of bubble formation at liquid–liquid interface.

1. $\sigma_{ab} > |\sigma_a - \sigma_b|$, the bubble is lenticular (Fig. 2B), and the minimum work of formation is given by Eq. [8] with

$$\sigma = [\sigma_a^3(\tfrac{1}{2} - \tfrac{3}{4}M_a + \tfrac{1}{4}M_a^3) + \sigma_b^3(\tfrac{1}{2} - \tfrac{3}{4}M_b + \tfrac{1}{4}M_b^3)]^{1/3}; \quad [10]$$

2. $\sigma_b \geq \sigma_a + \sigma_{ab}$, the bubble is spherical resting entirely within liquid a (Fig. 2A), and the minimum work of formation is given by Eq. [8] with

$$\sigma = \sigma_a; \text{ and} \quad [11]$$

3. $\sigma_a \geq \sigma_b + \sigma_{ab}$, the bubble is spherical resting entirely within liquid b (Fig. 2C), and the minimum work of formation is given by Eq. [8] with

$$\sigma = \sigma_b. \quad [12]$$

The criterion for bubble formation within liquid a corresponds to liquid a spreading on liquid b; while the criterion for bubble formation within liquid b corresponds to liquid b spreading on liquid a (10). The bubble is lenticular only if neither liquid spreads on the other. In such a situation it takes less work to create a lenticular bubble at the interface than a spherical bubble in either liquid.

Nucleation at the liquid–liquid interface in an emulsion always results in the lowest work of formation because both liquids can contribute to the vapor pressure in the bubble. If the bubble forms entirely in the more volatile liquid and the second liquid has a negligibly small vapor pressure, however, the additional work required to form the bubble away from the interface is quite small. As there are generally more sites in the bulk than at the interface, nucleation within the volatile liquid is the dominant process in such cases. In all other cases, where the work of bubble formation at the interface is substantially less than in either liquid, the dominant process is at the interface.

A bubble that is in thermal and mechanical equilibrium with the surrounding liquid is characterized completely by its composition, $(n_1'', n_2'', \ldots n_c'')$. Equation [8] represents the reversible work required to form such a bubble. However, this equation can be simplified. In many cases of practical interest σ_a and σ_b are insensitive to vapor composition, and the vapor can be treated as an ideal gas mixture. In this approximation

$$W(n_1'', n_2'', \ldots n_c'') = \frac{16}{3}\pi\sigma^3(p'' - p')^{-2} + \sum_i n_i''kT \ln \frac{p_i''}{p_i^*}. \quad [13]$$

In this equation σ depends only on the temperature, pressure, and composition of the liquids; k is Boltzmann's constant; T is the absolute temperature; p_i'' is the partial pressure of component i in the bubble ($p'' = \sum_i p_i''$); and p_i^* is the partial pressure of i when in chemical equilibrium with the surrounding liquid.

The volume of such a bubble is

$$V = \frac{32}{3}\pi\sigma^3(p'' - p')^{-3}. \quad [14]$$

Thus, the total number of molecules in the bubble, n'', is related to the total vapor pressure in the bubble as follows:

$$n'' = \left[\frac{32}{3}\pi\sigma^3(p'' - p')^{-3}\right]\frac{p''}{kT}. \quad [15]$$

Combining Eqs. [13] and [15] one obtains

$$W(n_1'', n_2'', \ldots n_c'') = W\dagger(n'') + \sum_i n_i''kT \ln \frac{y_i''}{y_i^*} \quad [16]$$

where

$$W\dagger(n'') = W\dagger(p'') = \left(\frac{32}{3}\pi\sigma^3(p'' - p')^{-3}\right) \times \left(\frac{1}{2}(p'' - p') + p'' \ln \frac{p''}{p^*}\right). \quad [17]$$

In Eq. [16] y_i'' is the mole fraction of component i in the bubble, and y_i^* is the equilibrium mole fraction of $i(y_i^* = n_i^*/n^* = p_i^*/p^*)$. Equation [16] reduces to the model of Jarvis *et al.* (10) when there is only one vapor species ($n'' = n_1''$).

The work of formation represented by Eq. [16] exhibits a saddle point when $p'' = p^*$ and $y_i'' = y_i^*$. This particular bubble is termed the nucleus. Its work of formation is

$$W^*(n_1^*, n_2^*, \ldots n_c^*) = \frac{16}{3}\pi\sigma^3(p^* - p')^{-2}. \quad [18]$$

where

$$p^* = \sum_i p_i^*.$$

This critical embryo plays a central role in determining the nucleation rate.

All bubbles grow by evaporation of molecules from the surrounding liquid. Neglecting for the time being the concurrent condensation process, the rate at which molecules of species i evaporate into a bubble is

$$\vec{k}_i = \beta_i S_i. \quad [19]$$

where $\beta_i = p_i^*(2\pi m_i kT)^{-1/2}$ is the maximum rate of evaporation per unit surface area, m_i is the mass of an i molecule, and S_i is the effective surface area of the bubble as seen by the i molecules.

The effective surface area, S_i, takes on different values depending on the relative position of the bubble with respect to the liquid–liquid interface. Assuming that the i species is present only in liquid a, we have three possibilities:

1. $\sigma_{ab} > |\sigma_a - \sigma_b|$, the bubble is lenticular (Fig. 2B), and

$$S_i = 8\pi\sigma_a^2(p'' - p')^{-2}(1 - M_a); \quad [20]$$

2. $\sigma_b \geq \sigma_a + \sigma_{ab}$, the bubble is spherical resting entirely within liquid a (Fig. 2A), and

$$S_i = 16\pi\sigma_a^2(p'' - p')^{-2}; \text{ and} \quad [21]$$

3. $\sigma_a \geq \sigma_b + \sigma_{ab}$, the bubble is spherical resting entirely within liquid b (Fig. 2C), and

$$S_i = \Delta_a. \quad [22]$$

This last case corresponds to what Jarvis *et al.* (10) term bubble blowing. Here, requirements of mechanical equilibrium force the bubble to rest entirely in liquid b while species i is assumed to be present entirely in liquid a. A definition for S_i in this situation must be rather inexact. In what follows we assume that Δ_a is equal to the average area occupied by a molecule in the liquid a/vapor interface. Errors in estimating this quantity have only a relatively small effect on the theoretical limit of superheat.

The above discussion proceeds in a similar fashion if species i is present only in liquid b, giving rise to the three situations:

1. $\sigma_{ab} > |\sigma_a - \sigma_b|$,

$$S_i = 8\pi\sigma_b^2(p'' - p')^{-2}(1 - M_b); \quad [23]$$

2. $\sigma_b \geq \sigma_a + \sigma_{ab}$, $S_i = \Delta_b$; and [24]

3. $\sigma_a \geq \sigma_b + \sigma_{ab}$,

$$S_i = 16\pi\sigma_b^2(p'' - p')^{-2}. \quad [25]$$

Now we are in a position to estimate the rate of bubble nucleation. If the absolute rates of evaporation and condensation which produce the various bubble species are much faster than the net rate of nucleation, the population of these bubbles should correspond closely to the predictions of equilibrium thermodynamics. At equilibrium (12)

$$X^{\mathrm{eq}}(n_1'', n_2'', \ldots n_c'') = N \exp(-W(n_1'', n_2'', \ldots n_c'')/kT), \quad [26]$$

where $X^{\mathrm{eq}}(n_1'', n_2'', \ldots n_c'')$ is the equilibrium number of bubbles having the composition $(n_1'', n_2'', \ldots n_c'')$, N is the total number of molecules in the liquid–liquid interfacial region when the dominant process is at the interface or the total number of molecules in the volatile liquid when the dominant process is in the bulk, and $W(n_1'', n_2'', \ldots n_c'')$ is given by Eq. [16].

The assumption that $X(n_1'', n_2'', \ldots n_c'') = X^{\mathrm{eq}}(n_1'', n_2'', \ldots n_c'')$ can never be valid for bubbles that are much larger than the critical nucleus because $W(n_1'', n_2'', \ldots n_c'')$

$\rightarrow -\infty$ when $n'' \rightarrow \infty$ for superheated systems. However, if this approximation is assumed valid for the nucleus, if every stable bubble that forms is assumed to pass through the nucleus state, and if any bubble that becomes larger than the nucleus is assumed to grow to macroscopic size with probability Γ, then an "equilibrium rate" estimate for the rate of nucleation can be obtained as

$$J = \Gamma(\sum_i \vec{k}_i) N \exp(-W^*/kT). \quad [27]$$

The utility of this expression lies in its simplicity. The surprising fact is that Eq. [27] with $\Gamma = 1$ yields reasonable estimates of superheat limits for both pure liquids and liquid–liquid emulsions.

In the next section we present a more detailed kinetic description of nucleation in emulsions of two pure liquids. This description yields a "steady-state" estimate for the rate of nucleation which can be cast in the same form as Eq. [27] and which provides an explicit expression for Γ.

3. RATE OF HOMOGENEOUS NUCLEATION

The actual stochastic process by which microscopic bubbles grow to macroscopic size can be modeled as a series of chemical reactions in which vapor bubbles are converted from one type embryo to another by addition or loss of single molecules from the surrounding liquid. When there is only one chemical species involved in these reactions, they take the form of a one-dimensional random walk or diffusion process. The steady-state kinetic treatment of such single component systems is well established and forms the basis of existing models for the rate of bubble nucleation. These theories assume that only one of the liquids in the emulsion exhibits an appreciable vapor pressure (10).

Kinetic treatment of systems in which there are more than one active component is more complicated. The problem was first studied by Reiss (13). He derived an expression for the steady-state rate of liquid droplet nucleation from a supersaturated binary vapor. The multicomponent generalization of Reiss's treatment was provided by Hirschfelder (14). Andres (15) also looked at this problem and extended the range of applicability of the Reiss–Hirschfelder formulation. In what follows we will for simplicity assume a binary system, i.e., an emulsion of two pure liquids. A general multicomponent formulation may be found in Ref. (15).

The net rate of a typical reaction step, $(n_a'',n_b'') \rightarrow (n_a''+1, n_b'')$, is

$$I_a(n_a'',n_b'') = \vec{k}_a(n_a'',n_b'')X(n_a'',n_b'') - \overleftarrow{k}_a(n_a''+1, n_b'')X(n_a''+1, n_b'') \quad [28]$$

where $X(n_a'',n_b'')$ is the number of bubbles with composition (n_a'',n_b''), $\overleftarrow{k}_a(n_a'',n_b'')$ is defined by Eq. [19], and $\overleftarrow{k}_a(n_a''+1, n_b'')$ is defined below in terms of $\vec{k}_a(n_a'',n_b'')$, $X^{\mathrm{eq}}(n_a'',n_b'')$, and $X^{\mathrm{eq}}(n_a''+1, n_b'')$. Making use of microscopic reversibility, one obtains

$$\frac{\vec{k}_a(n_a'',n_b'')}{\overleftarrow{k}_a(n_a''+1, n_b'')} = \frac{X^{\mathrm{eq}}(n_a''+1, n_b'')}{X^{\mathrm{eq}}(n_a'',n_b'')}. \quad [29]$$

Defining

$$f(n_a'',n_b'') = \frac{X(n_a'',n_b'')}{X^{\mathrm{eq}}(n_a'',n_b'')}, \quad [30]$$

Eq. [28] becomes

$$I_a(n_a'',n_b'') = \vec{k}_a(n_a'',n_b'')X^{\mathrm{eq}}(n_a'',n_b'') \times [f(n_a'',n_b'') - f(n_a''+1, n_b'')]. \quad [31]$$

When n_a^* and n_b^* are large, this expression can be approximated as (16)

$$I_a \simeq -\vec{k}_a X^{\mathrm{eq}} \frac{\partial f}{\partial n_a''}. \quad [32]$$

The net rate of increase of bubbles of species (n_a'',n_b'') is simply

$$\frac{dX(n_a'',n_b'')}{dt} = [I_a(n_a''-1, n_b'') - I_a(n_a'',n_b'') + I_b(n_a'', n_b''-1) - I_b(n_a'',n_b'')]. \quad [33]$$

If a pseudo steady-state is assumed and a continuous approximation to the discrete model is imposed (16), this equation becomes

$$\frac{\partial I_a}{\partial n_a''} + \frac{\partial I_b}{\partial n_b''} = 0. \quad [34]$$

Equation [34], along with the definitions for I, X^{eq}, and $\vec{k}$, given by Eqs. [32], [26], and [19], respectively, and the boundary conditions $f(0,0) = 1$ and $f(\infty,\infty) = 0$, completely define the steady-state nucleation problem. The key simplifications introduced by Reiss to obtain an analytical solution are: (a) all embryos that grow to macroscopic size pass through the region around the saddle point in the $W(n_a'',n_b'')$ surface; and (b) an orthogonal coordinate system (ζ_1,ζ_2) can be defined in this region so that the only nonvanishing component of the nucleation flux lies in the ζ_1 direction.

Introducing a general orthogonal transformation,

$$\begin{aligned} \zeta_1 &= \cos\phi n_a'' + \sin\phi n_b'', \\ \zeta_2 &= -\sin\phi n_a'' + \cos\phi n_b'', \end{aligned} \quad [35]$$

and assuming $I_2 = 0$, the flux in the ζ_1 direction at a fixed value of ζ_2 is (13–15)

$$I_1 = -\vec{k}_1 X^{\mathrm{eq}}(\zeta_1,\zeta_2)\frac{\partial f}{\partial \zeta_1}, \quad [36]$$

where

$$\vec{k}_1 = \frac{\vec{k}_a\vec{k}_b}{\vec{k}_a\sin^2\phi + \vec{k}_b\cos^2\phi}. \quad [37]$$

Integrating this expression along ζ_1, one obtains

$$-f(\zeta_1,\zeta_2)\Big|_{\zeta_1=0}^{\zeta_1=\infty} \simeq +1 = \int_0^\infty [\vec{k}_1 X^{\mathrm{eq}}(\zeta_1,\zeta_2)]^{-1} I_1 d\zeta_1. \quad [38]$$

The major contribution to this integral comes from the region near the nucleus. Assigning $\vec{k}_1$ and I_1 constant values in this region and removing them from the integral yields

$$I_1 \simeq \vec{k}_1 N \exp(-W^*/kT) \Big/ \times \int_{-\infty}^{\infty} \exp\left(\frac{W - W^*}{kT}\right) d(\zeta_1 - \zeta_1^*). \quad [39]$$

In the region near (ζ_1^*,ζ_2^*), $W(\zeta_1,\zeta_2)/kT$ can be expanded to yield

$$(W - W^*)/kT \simeq \frac{a_{11}}{2}(\zeta_1 - \zeta_1^*)^2 + a_{12}(\zeta_1 - \zeta_1^*)(\zeta_2 - \zeta_2^*) + \frac{a_{22}}{2}(\zeta_2 - \zeta_2^*)^2, \quad [40]$$

where $a_{11} < 0$ and $a_{22} > 0$. Substituting Eq. [40] into Eq. [39] and integrating yields

$$I_1 \simeq \vec{k}_1 N \exp(-W^*/kT)\left(\frac{|a_{11}|}{2\pi}\right)^{1/2} \times \exp\left[-\left(\frac{a_{22} + |a_{12}|}{2}\right)(\zeta_2 - \zeta_2^*)^2\right]. \quad [41]$$

Thus, the nucleation flux is

$$J = \int_0^\infty I_1 d\zeta_2 \simeq \vec{k}_1 N \exp(-W^*/kT) \times \left(\frac{|a_{11}|}{a_{22} + |a_{12}|}\right)^{1/2}. \quad [42]$$

Rewriting Eq. [42] in the form exhibited by Eq. [27], one obtains:

$$J \simeq \Gamma(\vec{k}_a + \vec{k}_b) N \exp(-W^*/kT), \quad [43]$$

where

$$\Gamma = \left(\frac{\vec{k}_1}{\vec{k}_a + \vec{k}_b}\right)\left(\frac{|a_{11}|}{a_{22} + |a_{12}|}\right)^{1/2}. \quad [44]$$

Before the steady-state nucleation rate can be calculated, we must derive explicit expressions for a_{11}, a_{12}, and a_{22} and determine the angle ϕ. From Eq. [16] the minimum work of forming a bubble is

$$W(n_a'',n_b'') = W^\dagger(n'') + n_a''kT\ln\frac{y_a''}{y_a^*} + n_b''kT\ln\frac{y_b''}{y_b^*}, \quad [45]$$

where $W^{\dagger}(n'')$ is given by Eq. [17]. Expanding this equation around (n_a^*, n_b^*) and introducing the coordinate transformation defined by Eq. [35], we obtain (15)

$$n^* a_{11} = \left(-\alpha + \frac{1}{y_a^*}\right) \cos^2 \phi - 2\alpha \sin \phi \cos \phi + \left(-\alpha + \frac{1}{y_b^*}\right) \sin^2 \phi, \quad [46]$$

$$n^* a_{12} = \left(\frac{y_a^* - y_b^*}{y_a^* y_b^*}\right) \sin \phi \cos \phi + \alpha(1 - 2 \cos^2 \phi), \quad [47]$$

$$n^* a_{22} = \left(-\alpha + \frac{1}{y_a^*}\right) \sin^2 \phi + 2\alpha \sin \phi \cos \phi + \left(-\alpha + \frac{1}{y_b^*}\right) \cos^2 \phi, \quad [48]$$

where

$$y_a^* \geq y_b^*,$$

and

$$\alpha = \frac{3p^*}{2p^* - p'} . \quad [49]$$

Thus, Γ is a function of p^* and p' through α, of y_a^* and $y_b^*(y_b^* = 1 - y_a^*)$, of $\vec{k}_a$ and $\vec{k}_b$, and of ϕ, where only the value of ϕ remains to be specified. Reiss (13) and later Hirschfelder (14) argued that ϕ should be chosen to diagonalize the Jacobian matrix

$$\left[\left. \frac{\partial^2 W/kT}{\partial n_a'' \partial n_b''} \right|_{n^*} \right] .$$

This is equivalent to picking ϕ so that $a_{12}(\phi) = 0$. Making use of Eq. [47] one obtains

$$\tan 2\phi = \frac{2\alpha}{(y_a^* - y_b^*)/(y_a^* y_b^*)} . \quad [50]$$

Andres (15) showed that this evaluation of ϕ is only valid when $\vec{k}_a = \vec{k}_b$. In general ϕ should be chosen so as to maximize $\Gamma(\phi)$. The values of ϕ and $\Gamma(\phi)$ obtained by these two approaches are compared in Sect. 5.

For most liquid systems a precise value of Γ is not necessary for estimating the maximum superheat. Thus, it is useful to develop and test simple approximations for Γ. The simplest model is, of course,

$$\Gamma = 1. \quad [51]$$

A more accurate approximation is to choose ϕ so that

$$\tan \phi = \frac{y_b^*}{y_a^*} , \quad [52]$$

and evaluate $\Gamma(\phi)$ using Eq. [44]. Still another approach is to estimate Γ by neglecting the volatility of one of the liquids when estimating the rate of nucleation. In this limit $(y_b^* = 0)$,

$$J = I_a = -\vec{k}_a N \exp(-W/kT) \frac{\partial f}{\partial n_a''} . \quad [53]$$

Integrating as before yields

$$J \simeq \vec{k}_a N \exp(-W^*/kT) \left(\frac{2\pi}{|a_{11}|}\right)^{1/2} . \quad [54]$$

Thus, Γ is equal to

$$\Gamma = \frac{\vec{k}_a}{\vec{k}_a + \vec{k}_b} \times \left(\frac{p_a^* - p'}{2p_a^* + p'}\right)^{1/2} (2\pi n_a^*)^{-1/2} . \quad [55]$$

This expression was obtained by Jarvis *et al.* (10).

In Sect. 5 we compare these various approximations for Γ with the more accurate model given by Eq. [44] in which ϕ is chosen to maximize $\Gamma(\phi)$. First, however, we describe a series of experiments designed to measure the nucleation temperatures or, more properly, the superheat limits of hydrocarbon/water emulsions. If these measurements reflect homogeneous nucleation at the hydrocarbon/water interface, Eqs. [43] and [44] should be able to predict the superheat limits that are observed.

4. EXPERIMENTAL METHOD AND OBSERVATIONS

The experimental method employed in the present work is a modification of the classical technique developed by Moore (3) and subsequently used by Eberhart *et al.* (6). A small drop (~1 mm diameter) of the desired emulsion is injected into the bottom of a column filled with a heavier immiscible, nonvolatile liquid (glycerine). The column is heated to produce a stable temperature profile which is hotter at the top than at the bottom. As the drop rises, it is heated until at some point bubble nucleation occurs. This method minimizes nucleation on solid surfaces and enables test emulsions to be heated above the boiling point of their continuous phase.

For the experiment to be meaningful there must be a higher probability for nucleation within the drop than at the interface between the drop and the surrounding liquid. As discussed in Sect. 2, this means that the continuous phase in the emulsion should spread on the nonvolatile liquid used in the column. Spreading occurred for the alkanes used in the present experiments when they contained a small amount of surfactant in solution (2% by volume). Glycerine is a questionable host liquid for superheating benzene, however. A drop of benzene containing surfactant spread initially on glycerine but ultimately formed a lens.

A schematic illustration of the apparatus is shown in Fig. 3. It consisted of a Pyrex tube 4.6 cm o.d., 4.0 cm i.d., and 60 cm long with rubber stoppers inserted at each end. The column was wrapped with 33 turns of No. 20 gage nichrome wire secured with Sauereisen cement. The wire spacing varied

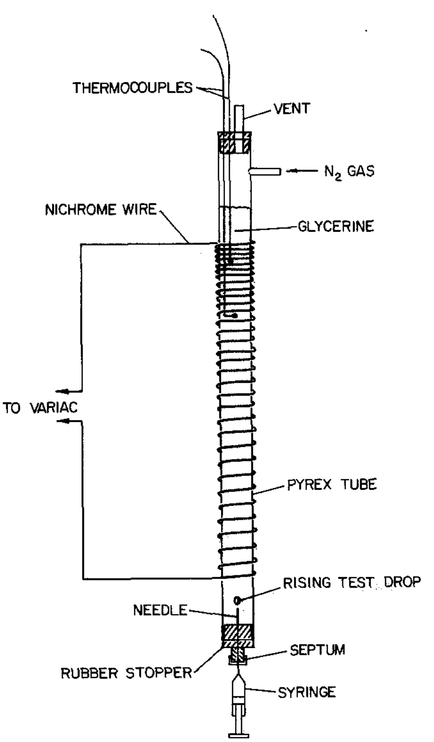

FIG. 3. Schematic of experimental apparatus.

from 2.5 cm at the bottom to 0.5 cm at the top. Power was provided by an ac current regulated by a Variac. Temperatures were measured by two No. 24 gage copper–constantan thermocouples enclosed in "L" shaped Pyrex tubes which were immersed directly into the glycerine. The thermocouples were connected to a Leeds & Northrup Model 8686 potentiometer and calibrated to about ±0.1°C.

A nitrogen atmosphere was maintained above the glycerine to reduce oxidation and subsequent darkening of the glycerine. All experiments were done at atmospheric pressure.

A small solid brass cylinder with a brass tube soldered on the end was fitted into a hole in the bottom rubber stopper. A 2 mm diam hole was drilled through the cylinder and a rubber septum was placed over the hole. Droplets were injected into the system through a No. 22 gage hypodermic needle, 5 cm long, which was inserted through the rubber septum.

An experiment consisted of stabilizing the temperature profile (requiring about 4 hr) and injecting 1 drop of the test emulsion. The drop slowly rises until a vapor bubble forms within it. At this point the drop rapidly vaporizes.

Attention was focused on a test section of approximately 10 cm in length near the top of the column. This region is just below the maximum temperature in the column and exhibits an almost linear temperature gradient of about 1°C/cm. The temperature in this section was adjusted until out of approximately 60 emulsion drops not one made it to the top of the column without vaporizing. While most of the drops vaporized before reaching the test section, several drops in each series vaporized in this region. The superheat limit of the emulsion was taken to be the temperature at the highest location in this test section where the latter drops vaporized.

Emulsions of water in benzene, *n*-decane, *n*-dodecane, *n*-tetradecane, and *n*-hexadecane, were tested. They contained approximately 83% by volume of the hydrocarbon, 15% water, and 2% surfactant. The emulsions were prepared in small samples of about 30 ml by first mixing the hydrocarbon with surfactant and then adding water and briskly agitating the mixture for about 10 min. The hydrocarbons were obtained from Humphrey Chemical Co. with a stated purity of 99.6% or better. The water was singly distilled. No special attempt was made to further purify the liquids other than normal filtering. The surfactants were mixtures of Span 85 and Tween 85 (alkane emulsions) and Span 80 and Tween 80 (benzene emulsions) available from Atlas Chemical Co. For the alkane/water emulsions HLB = 5.5 was used. HLB = 7.7 gave a stable benzene/water emulsion.

Difficulty in preparing stable emulsions was the greatest restriction we faced in studying a wider class of systems. The alkane/water emulsions stood for only a few minutes before visible separation occurred in the mixing beaker. The benzene/water emulsions lasted an average of 15 min before visible separation. Examination of the alkane/water emulsions under a microscope showed internal water droplet diameters ranging from 0.01 mm to 0.1 mm. Benzene/water emulsions exhibited more uniform water droplets of approximately 0.01 mm diameter.

In principle the dispersed water droplets are isolated in the hydrocarbon phase. In reality they settle slowly. This produces a clear region at the top of a rising emulsion drop. This settling also leads to substantial loss of water through the emulsion/glycerine interface. To minimize possible effects of this water loss on the column fluid, the glycerine was completely replaced after injection of approximately 100 drops. Often for small drops (<0.5 mm diameter) all the water disappeared from the emulsion before the test section was reached. The drop would then rise through the column usually without exploding. Therefore, data were taken only with drops of approximately 1 to 2 mm in diameter. These drops retained the majority of their water phase during transit through the column. They rose through the test section at a rate of approximately 8 cm/sec and could be assumed to be in thermal equilibrium with their surroundings.

The water/hydrocarbon mixtures appeared to be immiscible even at the temperatures involved in the nucleation experiments. Except for the settling phenomenon discussed above, the emulsions retained their milky appearance up to the point of explosion. We tested for miscibility by sequentially replacing the glycerine in the column with dodecane, tetradecane, and hexadecane and spraying water/surfactant solution into the top of the column through a 0.15 mm capillary. We could not detect any dissolving of the water drops as they fell through the column at temperatures in excess of 200°C. In addition to these observations, Dryer *et al.* (1) have used high speed photography to study burning *n*-dodecane/water drops suspended from a quartz fiber. Their observations indicate immiscibility of water and *n*-dodecane at the saturation temperature of *n*-dodecane (216°C).

Most of the emulsion drops vaporized before reaching the test section. For example, *n*-dodecane/water emulsions vaporized in a range of approximately 200–253°C and benzene/water emulsions nucleated in a range of approximately 140–201°C. The major cause of this scatter is thought to be the presence of microscopic air bubbles introduced during emulsion preparation. The vaporization of these drops occurs in the manner described by Sideman and Taitel (17). Because of their relatively slow rate of vaporization at the lowest temperatures in the column, drops containing visible air bubbles could easily be eliminated from consideration. Drops containing microscopic air bubbles, however, can reach relatively high levels in the column before disappearing as vapor and such events are easily confused with homogeneous nucleation.

The possibility exists that water loss to the glycerine phase gives rise to bubble nucleation near the boundary between the emulsion drop and the host fluid. Unfortunately, homogeneous nucleation measurements when the water/surfactant phase was sprayed directly into the hydrocarbon phase proved impractical. The initial disturbance of the drops as they hit the liquid surface and the tendency of the drops to collide with the walls of the column precluded careful homogeneous nucleation experiments with this configuration.

The emulsion drops did not explode in the sense of producing a "pop" or "bang" as do pure liquids. Instead they exhibited a sort of "breaking up" or "puffing" apart. This is indicative of the slower transport processes involved in rapid vaporization of an emulsion. The temperature dependence of the nucleation rate (Eqs. [43] and [44]), while still quite sharp, is also less abrupt than in the case of the pure liquids. Both of these phenomena tend to broaden the temperature range in which nucleation is observed.

The measured superheat limits of the hydrocarbon/water emulsions, T_m, are tabulated in Table I. These measurements are accurate to within ±2°C, although there

TABLE I

Comparison of Normal Boiling Temperatures of Various Pure Liquids with the Superheat Limits of Their Respective Water Emulsions

Emulsion	T_b	T_m	$T_c{}^a$	$T_c{}^b$
n-Decane/water	174	226	228	229
n-Dodecane/water	216	253	250	251
n-Tetradecane/water	252	253	259	260
n-Hexadecane/water	287	263	267	267
Benzene/water	80	201	211	212
Freon E-9/water	290	228[c]	231	232

[a] $\Gamma = 1$.
[b] Γ from Eq. [44].
[c] Jarvis *et al.* (10).

seems to be the chance for a systematic error in the benzene/water system.

Calibration runs with pure alkanes evidenced much less experimental scatter (i.e., nearly all the drops vaporized at one location in the test section). These experiments yielded superheat values identical to those in the literature to within ±1°C (7). Pure benzene exhibited greater experimental scatter than the alkanes. However, treating this data as with the emulsions (i.e., focusing on those drops that vaporize at the highest location in the test section) yielded a superheat limit identical to the accepted value (7).

5. DISCUSSION

Calculation of the superheat temperature of a binary emulsion from the formulations presented in Sect. 3 requires the following: (a) location of the nucleus relative to the liquid–liquid interface, (b) surface tension and vapor pressure of both liquids as a function of temperature, and (c) determination of what nucleation rate is commensurate with the experiment.

The nucleus position can be predicted by the criteria given in Sect. 2. To make this prediction, the interfacial tension between the two liquids as well as their individual surface tensions must be known. Jennings (18) has measured the interfacial tensions of benzene/water and *n*-decane/water systems to 176°C and Aveyard and Haydon (19) have reported dodecane/water, tetradecane/water, and hexadecane/water interfacial tensions up to 37.5°C. The effect of surfactant, however, is to lower this interfacial tension. We therefore tested the experimental systems to see whether the fuel (hydrocarbon + surfactant) spread on water. In all cases the hydrocarbon surfactant mixture (liquid b) spread on water (liquid a) at 25°C indicating that $\sigma_a > \sigma_b + \sigma_{ab}$. Assuming that spreading also occurs at high temperature, a spherical nucleus forms within the hydrocarbon as shown in Fig. 2C. This behavior should be quite general for fuel/water emulsions. The effective surface tension, σ, used in calculating W^* in such cases is the surface tension of the fuel, σ_b. This constitutes a great simplification in the theoretical treatment of these systems.

The effect of surfactant on the vapor pressure and surface tension of the hydrocarbon phase is believed to be small. This hypothesis was tested by determining the limit of superheat of drops of benzene and decane which contained surfactant. In both cases the superheat temperatures were the same as measured in the absence of surfactant. The possibility exists that neglect of the surfactant is no longer valid for the lower vapor pressure alkanes studied, but the superheat limits of these liquids were too high to be measured in our apparatus.

Because the calculations are so sensitive to surface tension, we list below the references from which we took surface tension data: (a) *n*-decane, Eberhart *et al.* (6); (b) *n*-hexadecane and *n*-tetradecane, Dickinson (20); (c) water, Volyak (21); and (d) benzene and *n*-dodecane, Jasper (22). The data of Jasper (22) were extrapolated to zero surface tension at the critical point.

Equilibrium vapor pressure data as a function of temperature were correlated by curve fitting the data of Gallant (23) and Weist *et al.* (24). The values of p_a^* and p_b^* used in Eq. [18] were obtained from the equilibrium vapor pressures, p_{ae}^* and p_{be}^*, by the relation (7)

$$(p_i^* - p') = \delta_i(p_{ie}^* - p'), \qquad [56]$$

where δ_i is the Poynting correction factor.

We assume droplet explosions are due to a single nucleation event inside the drop so that a nucleation rate corresponding to the total water/fuel surface area in a drop is appropriate. Following Eberhart *et al.* (6), the critical nucleation rate can be approximated as

$$J = \frac{dT}{dt} L \ln\left(\frac{N}{N_0}\right), \qquad [57]$$

where J is based on the total water/fuel interfacial area inside a drop. dT/dt (°C/sec) is the droplet heating rate. N/N_0 is the fraction of drops which survive to a temperature T, and L reflects the temperature dependence of the nucleation rate. From Eq. [43] it can be shown that J increases by a factor of about 20 per degree so that $L \approx 3$. Generally the mean nucleation temperature is defined so that $N/N_0 = ½$ (6). For an average emulsion drop diameter of 1.5 mm, the rate of rise in the column was measured to be about 8 cm/sec in a temperature gradient of 1°C/cm. Therefore, $dT/dt = 8$°C/sec. Assuming 15% by volume of water dispersed as individual droplets of 0.07 mm diameter, the total water/fuel interfacial area, A, per emulsion drop is 0.2 cm². Therefore from Eq. [57], $J/A \simeq 10^2$ nuclei/cm² sec.

In order to estimate N, we adopt a picture of the interface as comprising two molecular layers of thickness equal to the diameters of a water and fuel molecule, respectively. In this approximation

$$\frac{N}{A} = \bar{n}_a d_a + \bar{n}_b d_b, \qquad [58]$$

where d_a and d_b are effective diameters (cm) of water and fuel molecules respectively, and $\bar{n}_a$ and $\bar{n}_b$ are the number densities (molecules/cm³) of water and fuel.

We can now estimate emulsion superheat temperatures using Eq. [43]. The results are compared with our measured values in Table I. In Table I we also compare the measurement of Jarvis *et al.* (10) for a water drop rising in a column filled with Freon E-9 with our theoretical predictions. All temperatures are to the nearest degree. T_b is the normal boiling point of the fuel and T_m is the measured superheat limit of the emulsion. $T_c{}^a$ is the predicted temperature using $\Gamma = 1$ in Eq. [43] and $T_c{}^b$ is the temperature calculated using the more refined steady-state value for Γ (Eq. [44]). Several approximations were used to estimate ϕ in this last calculation. The various superheat temperatures were so close, however, that only one temperature is listed.

We consider the agreement between the highest measured temperatures and the calculated temperatures quite good. Moreover, the predicted temperatures using the simplified equilibrium model with $\Gamma = 1$ and the refined steady-state model are essentially the same. This is due to the predominant dependence of the nucleation rate on the exponential term, $\exp[-W^*/kT]$, which is the same in both cases.

The differences between the various models for ϕ and for Γ presented in Sect. 3 are illustrated in Table II. The temperature at which the calculations were made is indicated in the first column. Because of its importance in differentiating between the Andres (15) formulation and the Reiss–Hirschfelder (13, 14) formulation, the ratio $\vec{k}_b/\vec{k}_a$ is also given. The differences between these models is small unless $\vec{k}_b/\vec{k}_a$ is very different from unity. The predictions of the two models are indistinguishable for the emulsions we studied with the single exception of benzene/water. The predictions of Eq. [52] are also very close to those of the Reiss–Hirschfelder model (Eq. [50]). There is not much added computational effort involved in using the Reiss–Hirschfelder value for ϕ for binary systems. The generalization of Eq. [52] to multicomponent systems, however, is much simpler as it involves determination of the direction of a ray from the point (0,0,0 . . . 0) to the point $(n_1^*, n_2^*, \ldots, n_c^*)$ while the Reiss–Hirschfelder approach involves evaluation of the eigenvalues of a $c \times c$ dimension Jacobian matrix.

Finally, it is apparent that the value of Γ obtained by assuming $y_b^* = 0$ is too low for the emulsions studied.

Table II shows that differences in Γ and hence the predicted nucleation rate at a given temperature can be significant. The effect of such differences on the critical superheat limit is nevertheless small. This

TABLE II

Comparison of Theoretical Estimates of ϕ and Γ

Emulsion	T (°C)	$\hat{k}_b/\hat{k}_a$	ϕ^a	Γ^a	ϕ^b	Γ^b	ϕ^c	Γ^c	Γ^d
n-Decane/water	229.4	16.7	10.6	0.0168	10.6	0.0168	7.4	0.0157	0.00147
n-Dodecane/water	250.7	5.0	4.5	0.0290	4.5	0.0290	3.0	0.0282	0.00447
n-Tetradecane/water	260.1	2.3	2.4	0.0372	2.4	0.0372	1.6	0.0367	0.00814
n-Hexadecane/water	267.4	1.0	1.2	0.0426	1.2	0.0426	0.8	0.0423	0.0137
Benzene-water	212.3	132.0	71.7	0.0208	41.9	0.00924	40.5	0.00868	0.000196
Freon E-9/water	231.5	0.2	0.4	0.0405	0.4	0.0405	0.3	0.0404	0.0223

[a] Andres model, ϕ which maximizes Γ.
[b] ϕ from Eq. [50].
[c] ϕ from Eq. [52].
[d] Γ from Eq. [55].

same phenomenon should carry over in the case of bubble nucleation in multicomponent miscible mixtures. It is no wonder that single component homogeneous nucleation formulations have been used with some success in estimating superheat temperatures in systems with two active species (25). The critical modification required is to use the proper effective surface tension and to sum the partial pressures of the vapor species when evaluating W^*/kT.

A simple working formula to predict the superheat limits of fuel/water emulsions in flames can be based on the energy required to form a critical size nucleus at the fuel/water interface (Fig. 2C). A best fit of our experimental measurements yields

$$\frac{W^*}{kT_c} = \frac{16\pi\sigma_b{}^3(T_c)}{3kT_c(p_a{}^*(T_c) + p_b{}^*(T_c) - p')^2} = 66, \qquad [59]$$

with $p' = 1$ atm.

The ability of this expression to correlate our measurements is shown in Fig. 4. Any systems falling within the region $T_c/T_b < 1$ in Fig. 4 should burn disruptively at atmospheric pressure.

It is important to remember that there may be many drops that vaporize disruptively at lower temperatures than T_c. The presence of microscopic air bubbles in emulsified fuel drops can cause premature vaporization. Solid particles or surfaces can also promote nucleation. An example of this latter phenomenon is the observed disruptive burning of dodecane/water emulsion drops suspended from a quartz fiber (1). The predictions of homogeneous nucleation theory and our measurements indicate that a free burning dodecane/water drop will not undergo a microexplosion at atmospheric pressure.

It is also important to note that the presence of a superheated water phase within a fuel drop does not mean that the drop will vaporize disruptively. The driving force for a microexplosion is present but there is a nucleation barrier that must be overcome before disruptive vaporization occurs.

Equation [59] can be used to predict the *maximum* nucleation temperatures of fuel/water emulsions if the surface tension and vapor pressure of the fuel phase are known. Systems where $T_c/T_b < 1$ will burn disruptively even in the absence of air bubbles or solid particles.

CONCLUSIONS

Maximum superheat temperatures of emulsion drops measured using the column heating method can be predicted by means of homogeneous nucleation theory. The hydrocarbon/water emulsions studied here correspond to a very low interfacial tension

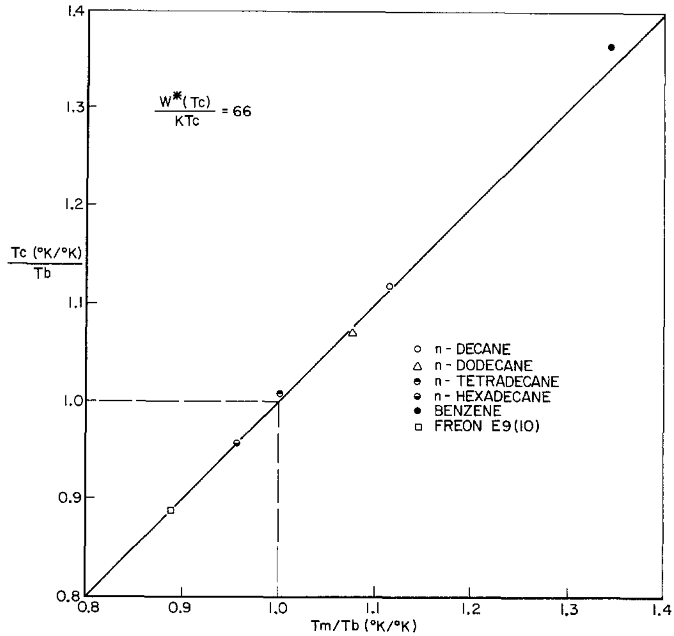

FIG. 4. Comparison for some fuel/water emulsions of the highest measured superheat temperatures, T_m, with temperatures calculated by using $W^*/kT_c = 66$.

and to a spherical nucleus forming at the hydrocarbon/water interface but surrounded by the hydrocarbon phase.

There is little difference between superheat limits calculated using a simple equilibrium rate model for nucleation and calculated using a steady-state rate formulation. The differences in the absolute nucleation rate calculated from these two models can, however, be significant.

Based on the superheat limits measured, only the hexadecane/water emulsions should burn disruptively via homogeneous nucleation at 1 atm. The *n*-decane, *n*-dodecane, *n*-tetradecane, and benzene emulsions all have nucleation temperatures higher than the boiling points of the respective fuel. There were differences in the explosive character of these emulsions. They ranged from an inaudible "puff" in the alkane/water emulsions to a sharp report in the benzene/water system. These differences are indicative of the relative rates of the transport processes involved in these microexplosions.

Maximum superheat temperatures of the emulsions are well correlated by $W^*/kT_c = 66$. Temperatures calculated from this correlation are the highest one should expect an emulsified fuel droplet to reach at atmospheric pressure.

ACKNOWLEDGMENTS

We are sincerely grateful to I. Glassman for introducing us to the interesting behavior of emulsified fuels and for his support and advice given throughout the course of the work. Conversations with F. L. Dryer, C. K. Law, D. W. Naeglie, and R. J. Santoro have also been helpful. Financial support for R. P. Andres was provided under NSF Grant GK-4160. The experimental efforts and the work of C. T. Avedisian, an NSF trainee, was supported by NSF/RANN Grant AER 76-08210 (I. Glassman/F. L. Dryer, Principal Investigators), which is monitored by the Division of Conservation Research and Technology, ERDA. All support is gratefully acknowledged.

REFERENCES

1. Dryer, F. L., Report No. 1224, Department of Aerospace and Mechanical Sciences, Princeton University, April 1975; Dryer, F. L., Rambach, G. D., and Glassman, I., Report No. 1271,

Dept. of Aero. and Mech. Sci., Princeton Univ., Apr. 1976.
2. Ivanov, V. M., and Nefedov, P. I., NASA Technical Translation NASA TT F-258, Jan. 1965.
3. Moore, G. R., *AIChE J.* **5,** 458 (1959); Ph.D. thesis, University of Wisconsin (1956); (Publication 17,330, Univ. Microfilms, Ann Arbor, Mich.).
4. Blander, M., Hengstenberg, D., and Katz, J. L., *J. Phys. Chem.* **75,** 3613 (1971).
5. Kagan, Y., *Russ. J. Phys. Chem.* **34,** 42 (1960).
6. Eberhart, J. G., Kremsner, W., and Blander, M., *J. Colloid Interface Sci.* **50,** 369 (1975).
7. Blander, M., and Katz, J. L., *AIChE J.* **21,** 833 (1975).
8. Porteous, W., and Blander, M., *AIChE J.* **21,** 560 (1975).
9. Apfel, R. E., Harvard University Acoustics Research Laboratory, Technical Memorandum 62, Feb. 1970; *J. Chem. Phys.* **54,** 62 (1971).
10. Jarvis, T. J., Donohue, M. D., and Katz, J. L., *J. Colloid Interface Sci.* **50,** 359 (1975).
11. "The Collected Works of J. Willard Gibbs", Vol. 1, p. 260. Longmans, Green, New York, 1928.
12. Frenkel, J., "Kinetic Theory of Liquids," p. 384. Oxford Univ. Press, London, 1946.
13. Reiss, H., *J. Chem. Phys.* **18,** 840 (1950).
14. Hirschfelder, J. O., *J. Chem. Phys.* **61,** 2690 (1974).
15. Andres, R. P., *J. Chem. Phys.*, submitted for publication (1978).
16. Cohen, E. R., *J. Statistical Phys.* **2,** 147 (1970).
17. Sideman, S., and Taitel, Y., *Int. J. Heat Mass Transfer* **7,** 1273 (1964).
18. Jennings, H. Y., *J. Colloid Interface Sci.* **24,** 323 (1967).
19. Aveyard, R., and Haydon, D. A., *Trans. Faraday Soc.* **61,** 2255 (1965).
20. Dickinson, E., *J. Colloid Interface Sci.* **53,** 467 (1975).
21. Volyak, L. D., *Dokl. Akad. Nauk, SSSR* **74,** 307 (1950).
22. Jasper, J. J., *J. Phys. Chem. Ref. Data* **1,** 841 (1972).
23. Gallant, R. W., "Physical Properties of Hydrocarbons," Vol. 1. Gulf Publ., Houston, 1968.
24. "Handbook of Chemistry and Physics" (R. C. Weist, S. M. Selby, and C. D. Hodgman, Eds.), 46th ed., Chem. Rubber, Cleveland, 1965.
25. Mori, Y., and Nagatani, T., *Int. J. Heat Mass Transfer* **19,** 1153 (1976).